Available online at www.sciencedirect.com

ScienceDirect

Cement and Concrete Research 37 (2007) 492–501

Cement and Concrete Research

# Crystallisation of calcium hydroxide in early age model and ordinary cementitious systems

E. Gallucci *, K. Scrivener

*Laboratory of Construction Materials, Ecole Polytechnique Fédérale de Lausanne, CH-1015, Switzerland*

Received 29 August 2006; accepted 10 January 2007

**Abstract**

The distribution and morphology of CH particles in various cementitious systems was investigated to determine which parameters influence their nucleation and growth. Morphological image analysis of SEM-BSE images of polished cross-sections was used to measure CH distribution, particle size and shape within the microstructure. It was observed that CH crystallises according to two main patterns, the first consisting of a few, large, convoluted and unevenly distributed clusters, while the second consists of numerous smaller particles, evenly and closely distributed in the matrix. The growth of CH in Portland cement type systems seems to be the result of a specific interaction between the availability of gypsum and alumina, with CH crystals nucleating in the vicinity of gypsum particles.

*Keywords:* Calcium hydroxide; Cementitious systems; SEM; Image analysis

## 1. Introduction

Calcium hydroxide (CH) or portlandite is well known as one of the main products of cement hydration, along with C–S–H. Although extensive work has been done on the hydration of Portland cement (PC) as well as on blended systems, the formation of CH has received relatively little attention compared to other hydrate phases. It is well recognised that CH plays a critical role in buffering the pH of the pore solution, so protecting reinforcement from corrosion. On the other hand, it is implicated in the formation of efflorescence and is considered to be more susceptible to leaching. A good review on the properties of CH can be found in the special volume of *Materials Science of Concrete* especially dedicated to calcium hydroxide [1].

From a microstructural point of view, several issues such as the crystallinity of CH, its growth and the size, morphology and distribution of clusters in the microstructure have to be considered. Glasser [2] identifies two types of CH in PC: the first corresponds to physically discrete crystallites and the second to labile particles initially present in C–S–H gel with high Ca/Si ratio and responsible for its capability to donate calcium [3,4]. Several authors have proposed that the structure of C–S–H could consist of the intermixing of tobermorite-like or jennite-like structural units with continuous protolayers of CH [5–9].

Although the existence of amorphous or microcrystalline CH in C–S–H seems established, the vast majority of this phase in cementitious systems occurs in the form of micrometer-sized crystals. Depending on the hydration conditions, CH in PC is known to occur as massive clusters and/or as isolated hexagonal crystals. However, there have been very few systematic studies of the nucleation and growth of these crystals, either in terms of their size and spatial distribution or of the way this is influenced by the growth environment. Only two previous publications could be found concerning these aspects: Diamond [10] investigated the morphology of CH clusters in 3- and 100-day-old pastes by means of SEM image analysis. He concluded that CH exists as discrete particles with a mean size distribution of 7 μm, that none of these particles were euhedral (hexagonal platelet-like) and that the growth of CH is constrained and limited by the tortuous free space available.

---

* Corresponding author.
*E-mail address:* emmanuel.gallucci@epfl.ch (E. Gallucci).

0008-8846/$ - see front matter © 2007 Elsevier Ltd. All rights reserved.
doi:10.1016/j.cemconres.2007.01.001

Kjellsen and Justnes [11] reported on the microstructure of hydrated pure $C_3S$ pastes. Although PC contains about 70% of $C_3S$, the microstructure of $C_3S$ pastes differs significantly from that of cement pastes. They suggested that the morphological differences of CH in $C_3S$ and PC (respectively, large concentrated masses vs. finely dispersed particles with complex and irregular shapes) could be attributed to the difference in pH of the systems although they did not look at this effect in their study. Kjellsen and Justnes [11] suggested that the ions present as impurities in alite (impure form of $C_3S$) induce more abundant CH nuclei in PC than in $C_3S$. However, although they used Mg- and Al-stabilised alite instead of pure $C_3S$, the number of CH nuclei remained limited. To date, none of the hypotheses advanced to explain the variations of CH morphology have been validated experimentally.

The present study looks at the distribution and morphology of CH in various cementitious systems in order to assess which parameters influence its nucleation and growth. Polished sections of pastes aged from a few hours to several days were prepared for SEM backscattered electron (BSE) imaging. Morphological image analysis was used to measure CH distribution, particle size and shape within the microstructure. The differences observed are discussed and correlated with the chemical environment of ions in solution in the fresh cement pastes.

## 2. Materials and methods

Several hydrated systems ranging from pure tricalcium silicate ($C_3S$—the main phase of PC) to PC were prepared and examined (Tables 1 and 2). The pure phases $C_3S$ and $C_3A$ were synthesised by several heating/grinding cycles of stoichiometric mixes of pure reagent grade reactants: $CaCO_3$ and $SiO_2$ at 1650 °C for $C_3S$ and $CaCO_3$ and $Al_2O_3$ at 1050 °C for $C_3A$. In the case of polyphase systems of $C_3S$ and $C_3A$, the two phases were produced and sintered together at 1500 °C. The purity of the synthesised phases was checked by means of X-ray diffraction and glycol titration.

The raw materials were mixed and hand ground for a few minutes before the addition of water. The synthetic gypsum used in the model systems was observed to be slightly coarser than in PC since the grinding process in cement plants is much more efficient. The hydrated systems were prepared at a water to cement ratio of 0.4 and hydration was stopped at different ages ranging from a few hours to several days. Prior to SEM examination, samples were dried, impregnated and polished. At early ages (before 24 h of hydration), a large part of the water is still unbound (i.e. has not yet reacted) and has to be removed. This was done by freeze-drying (freezing of the free water in a −80 °C cold mix of ethanol and solid $CO_2$—drying by sublimation). Water in older samples was removed by solvent exchange in propan-2-ol for one week. Once dried, specimens were impregnated under vacuum in an epoxy resin (EPOTEK 301) and gently polished with decreasing grades of diamond powders down to 1/4 µm.

Table 1
Mix design of studied systems (in grams)

| System | Type | $C_3S$ | $C_3A$ | C$ | Water |
|---|---|---|---|---|---|
| 1 | Monophased | 100 | – | – | 40 |
| 2 | Monophased | 95 | – | 5 | 40 |
| 3 | Monophased | 100 | – | – | 40 (0.1 M KOH) |
| 4 | Monophased | 95 | – | 5 | 40 (0.1 M KOH) |
| 5 | Monophased | 73* | 18 | 9 | 40 |
| 6 | Polyphased | 73* | 18 | 9 | 40 |
| 7 | Portland cement | 100 (see Table 2) | | | 40 |

*Alite.

Table 2
Studied OPC

Cement type : CEM I 42.5

Composition as determined by XRD-Rietveld (mass %)

| | | | | | |
|---|---|---|---|---|---|
| $C_3S$—a | 71.03 | $C_3A$—o | 01.57 | $CaSO_4 \cdot 2H_2O$ | 04.45 |
| $C_2S$—b | 06.02 | CaO | 00.65 | $CaSO_4 \cdot 1/2H_2O$ | 00.55 |
| $C_4AF$ | 09.50 | MgO | 00.42 | $CaSO_4$ | 00.91 |
| $C_3A$—c | 02.33 | $CaCO_3$ | 02.53 | | |

a—alite; b—belite; c—cubic; o—orthorhombic.

The polished sections were studied in backscattered electron (BSE) mode using an FEI quanta 200 SEM at an accelerating voltage of 15 kV. Image analysis was used to identify differences between the systems and to gain insight on CH morphology, in order to assess how the different factors influence its development in cementitious materials.

BSE generate a specific phase contrast, thanks to which phases can be identified according to their brightness in the image, those with the greatest average atomic number being the brightest, and those with the lower atomic number being darker. This allows the components of the microstructure to be discriminated on the basis of the grey level histogram (distribution of the grey levels of all pixels). With regard to CH clusters, the first morphological parameter of interest is their size distribution. Because of the complicated and tortuous shapes of CH in cementitious systems, the concept of 'size' is not trivial as it requires definition by more than one parameter. The Feret lengths – distance between two tangents on opposite sides of the particle – and particularly the Feret diameter (mean of several Feret lengths) which minimise the influence of the shape of particles on the measured value [12]. As the morphology and shape of CH is significantly different between the $C_3S$ and the PC cases, another parameter of interest to characterise CH was the circularity or its inverse, the form factor. A circle has a circularity of 1, objects having irregular shapes have a circularity higher than 1. The circularity and the form factor are calculated according to the following formulae,

$$\text{circularity } C = \frac{\text{perimeter}^2}{4 \cdot \pi \cdot \text{area}} \qquad \text{form factor } F = \frac{1}{\text{circularity}}.$$

The final morphological parameter studied here is the distribution of CH particles within the cementitious matrix which was evaluated by averaging the distances between each particle and its nearest neighbours. The mean distance between all pairs of closest centroids gives an indication of the distribution of CH nucleation points in the material. It is well appreciated that these morphological parameters are derived on two-dimensional sections of a three-dimensional microstructure; nevertheless, the 2D parameters are valid for comparative purposes and no attempt is made to convert the parameters to the 3D case as this is problematic due to the need for model assumptions.

These morphological parameters were measured for the 7 systems in Table 1. For each of them, 80 to 100 different fields at a magnification of ×800 (pixel size of 0.362 μm) were analysed in order to minimise the influence of local variations and to give a statistically representative characterisation of the microstructure.

## 3. Results and discussion

### 3.1. Nucleation and growth of CH in the early stages of hydration of $C_3S$ and PC

After 1 day of hydration, the difference between the $C_3S$ and PC systems is clearly established as illustrated in Fig. 1. As reported by Kjellsen and Justnes [11], CH in $C_3S$ grows only from a few nuclei and rapidly extends into very large clusters which totally envelop $C_3S$ grains, preventing their further hydration. At later stages of hydration, CH seems to grow preferentially on the existing clusters rather than elsewhere in the matrix. The development of CH in PC is radically different: numerous CH particles with various shapes and sizes are observed throughout the matrix. One of the main differences compared to the $C_3S$ system is the presence of long thin CH crystals randomly distributed in the microstructure; these are the cross section of CH platelets which extend above and below the sampling plane [13]. Diamond [10] suggested that these particles are elongated because they precipitate in narrow spaces between the partially reacted cement grains. However, after only a few hours of hydration, these 'elongated' CH particles are already present although their growth is not constrained by limited space.

The microstructural development was followed from 4 to 16 h to study the nucleation and growth of CH in these two systems. Characteristic SEM micrographs are given in Fig. 2.

After 4 h of hydration, there are few signs of reaction in the $C_3S$ system: the shape of the grains does not appear to be altered by reaction and there is no sign of C–S–H on their surfaces. However, the existence of a few isolated small CH clusters confirms that the hydration has started. By 8 h, there is little change except that more CH clusters are observed and these

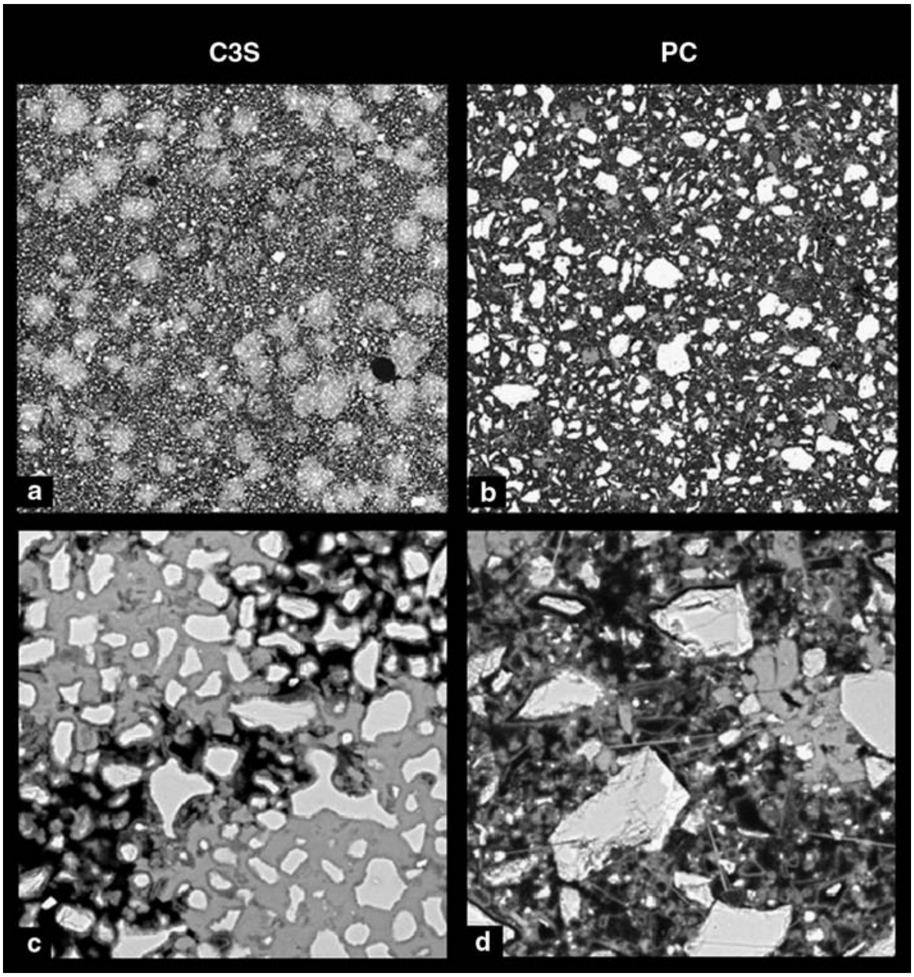

Fig. 1. One day hydration of $C_3S$ and OPC pastes (scale—full width: a and b: 900 μm; c and d: 80 μm).

have grown significantly, already encapsulating unreacted grains. After 16 h of hydration, thin rims of C–S–H are seen around the reacting grains; very large CH clusters infiltrate the matrix enclosing large numbers of unreacted grains. The most recent grains to be engulfed (i.e. those which are on at the outer border of the CH clusters) are surrounded by rims of C–S–H. As already mentioned, CH tends to grow onto existing clusters rather than precipitating new crystals in the microstructure.

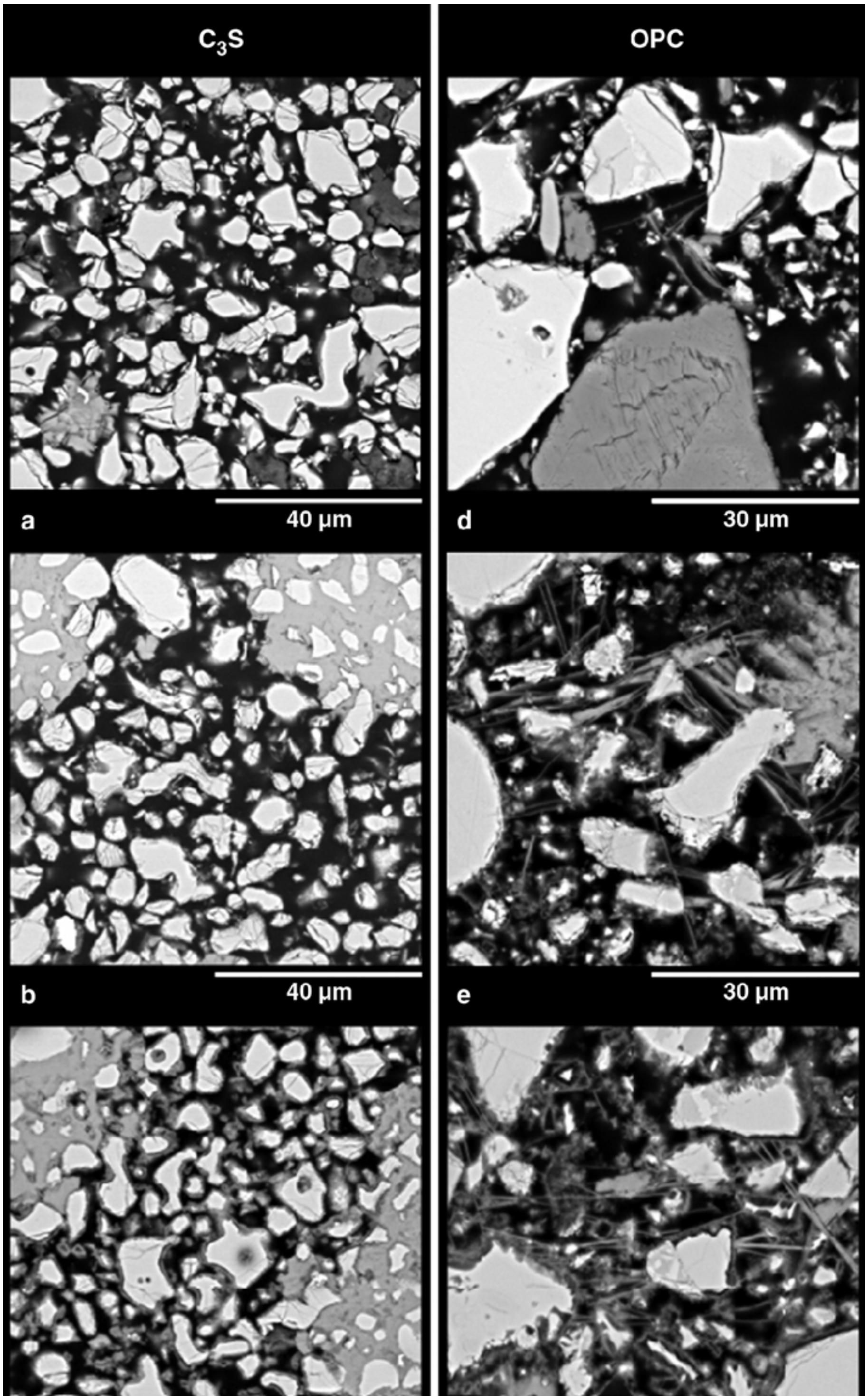

Fig. 2. Growth of CH in early age $C_3S$ and OPC pastes (a and d: 4 h; b and e: 8 h; c and f: 16 h).

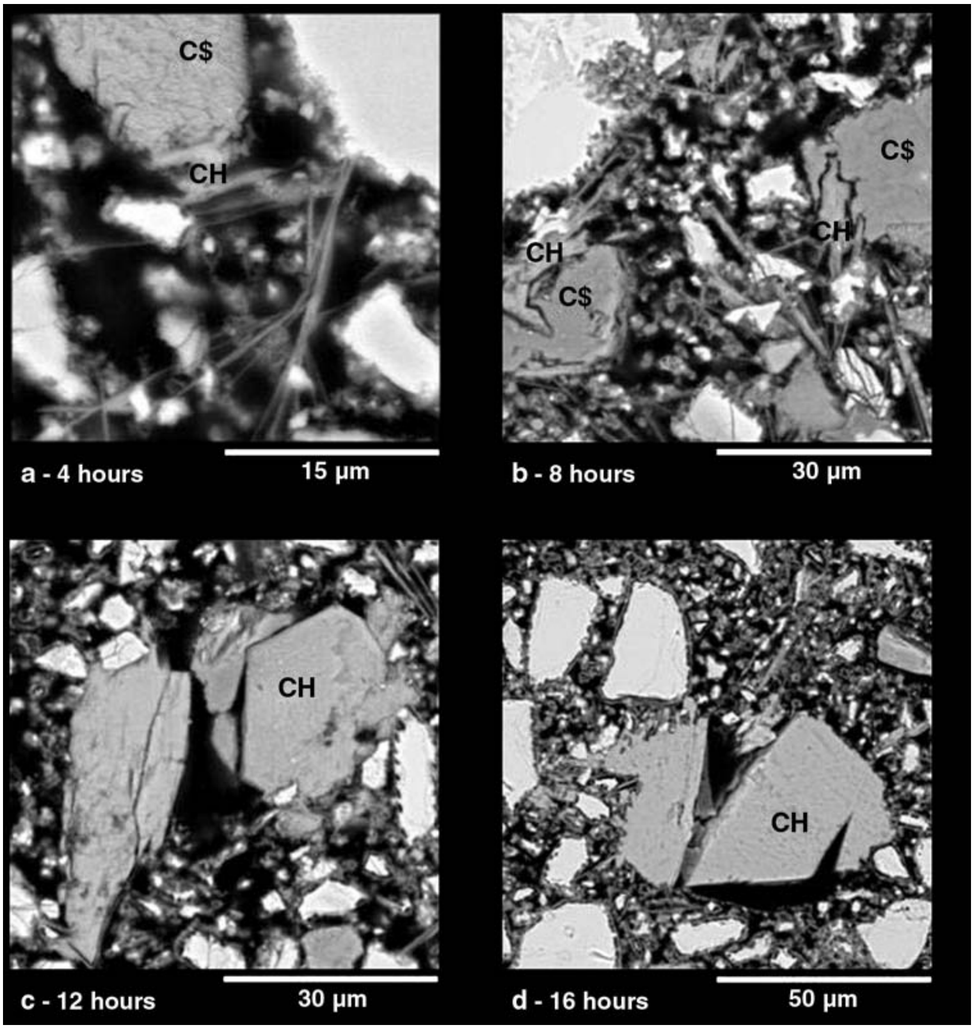

Fig. 3. Relation between CH and calcium sulfate in early age OPC pastes.

In PC (Fig. 2), the first occurrence of CH is observed at 4 h in the neighbourhood of gypsum grains. At 8 h, while very little C–S–H has precipitated, more CH has formed and the platelets appear to bridge between the cement grains. At later ages, when the hydration reaction has advanced further, a complex network of connected CH platelets can be seen. By 16 h, large amounts

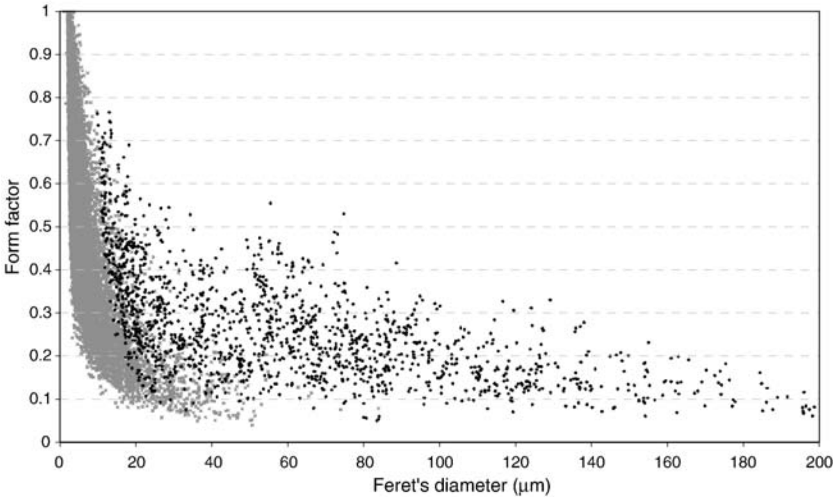

Fig. 4. Form factor vs. particle size (grey: OPC; black: $C_3S$).

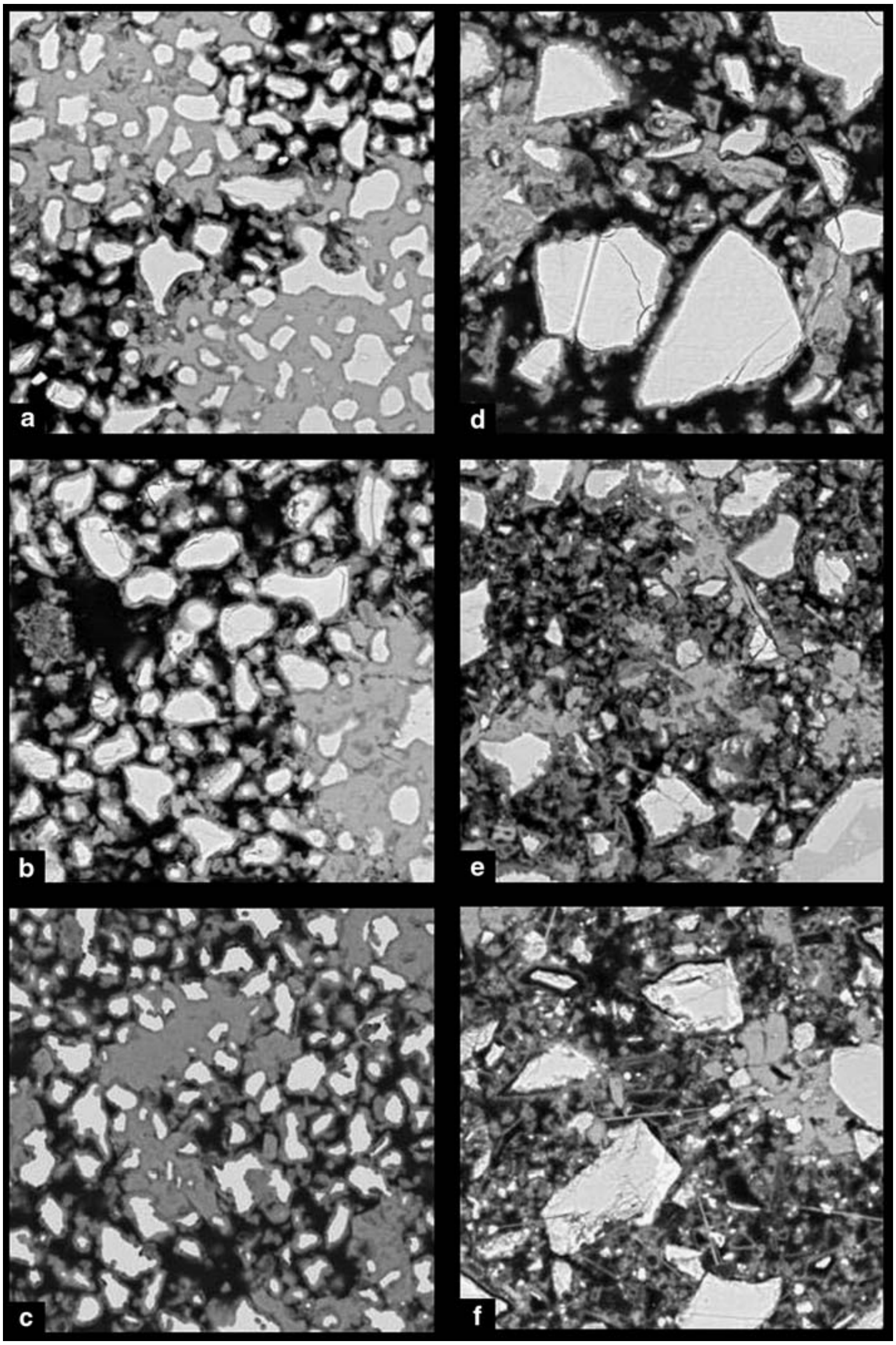

Fig. 5. General microstructure of the studied systems after 1 day of hydration (scale: full width = 80 μm). (a) system 1: $C_3S$; (b) system 2: $C_3S + C\$$; (c) system 3: $C_3S$-C\$-alk; (d) system 5: M-$C_3S$-$C_3A$-C\$; (e) system 6: P-$C_3S$-$C_3A$-C\$; (f) system 7: OPC.

of C–S–H have precipitated on all solid phases present which act as a support for heterogeneous nucleation. The nucleation of CH seems to be favoured in the neighbourhood of gypsum grains: for instance in Fig. 3a, the rough (i.e. reacting) end of the gypsum grain seems to be the starting point of a CH particle. At later ages, the growth of CH clusters in the vicinity of gypsum is clearer as seen in Fig. 3b: coarser gypsum grains react slowly and it appears that the free space created is filled with CH. After 16 h, the biggest gypsum grains have almost totally reacted, and large CH clusters seem to grow in their place. The morphology of such clusters shows characteristic angles of 120° (Fig. 3c and d), in agreement with the well known hexagonal crystal structure of CH.

The data on the particle morphology for the two systems at one day are given in Fig. 4 which shows quite discrete results with almost no overlap of the data. Most of the CH particles in PC have a size smaller than 20 microns while for $C_3S$, this corresponds to the minimum measured size. For particles of comparable size, $C_3S$ shows much higher form factors (i.e. particles are more circular) than PC. In the case of PC, the smallest particles are distributed over a wide range of form factors ranging from values close to 1 (rounded particles) down

Table 3
Morphological image analysis

| | System | Hydration degree (%) | CH content (mass %) | nb CH clusters[a] | Mean Feret's diameter (µm)[b] | Median form factor[b] | Mean free distance (µm) |
|---|---|---|---|---|---|---|---|
| 1 day | 1. $C_3S$ | 45.86±3.58 | 21.18±2.87 | 010 | 60 | 0.19 | 74±67 |
| | 2. $C_3S$–C$ | 47.67±3.42 | 21.89±2.45 | 013 | 58 | 0.23 | 51±35 |
| | 3. $C_3S$–alk | 54.39±2.33 | 21.41±2.71 | 013 | 55 | 0.26 | 66±30 |
| | 4. $C_3S$–C$–alk | | | 022 | 33 | 0.24 | 46±18 |
| | 5. M–$C_3S$–$C_3A$–C$ | 51.44±4.41 | 10.49±1.24 | 101 | 09 | 0.61 | 15±18 |
| | 6. P–$C_3S$–$C_3A$–C$ | 46.74±3.94 | 12.99±1.38 | 183 | 08 | 0.52 | 13±06 |
| | 7. Portland cement | 40.30±3.47 | 10.94±1.32 | 176 | 07 | 0.62 | 12±06 |
| 7 days | 1. $C_3S$ | 62.81±3.81 | 20.97±3.41 | 033 | 72 | 0.25 | 75±68 |
| | 7. Portland cement | 66.09±3.50 | 13.09±1.59 | 322 | 19 | 0.54 | 15±13 |
| 28 days | 1. $C_3S$ | 83.11±2.71 | 21.49±2.59 | 034 | 69 | 0.23 | 71±67 |
| | 7. Portland cement | 74.07±4.10 | 20.02±2.42 | 315 | 19 | 0.48 | 12±11 |

[a] Mean number of CH clusters by unit field.

[b] Mean or median values form large distributions, to be considered as indicator of trends rather than absolute measurement.

to very low values for elongated particles (which correspond to thin hexagonal platelets in 3D). Regarding large particles, the trend is the same in both systems that show a decreasing form factor with an increasing cluster size; this is mainly due to the spatial constraints of the neighbouring particles.

The microstructural development of these two systems is thus significantly different from the very early stages of hydration, although PC is made of 70% of $C_3S$. The differences between the two systems must be caused by the other species present such as sulfates, aluminate phase ($C_3A$) or alkali ions. From these observations we have an indication that calcium sulfate particles seem to act as nuclei of CH clusters or at least, their neighbourhood favours the crystallisation of CH.

### *3.2. Influence of calcium sulfates, calcium aluminate phases and alkali ions*

In order to understand the observed differences and to assess if calcium sulfate does play a role in the crystallisation of CH, systems ranging from pure $C_3S$ to PC were studied (systems 2–6). These systems are combinations of $C_3S$ or alite with controlled amounts of calcium sulfate, calcium aluminate and alkali, as detailed in Table 1. Characteristic micrographs are shown in Fig. 5, from these images it can be seen that the systems can be classified into two main categories (from the point of view of CH characteristics).

This is confirmed by the numerical results given in Table 3. Within each sample there is a considerable range of variation between individual CH particles (partly due to sectioning effects). Therefore, Table 3 gives just the median values as a broad *characteristic* of the system to help differentiate them from each other. After 1 day of hydration, the morphological parameters clearly differentiate the systems into two types: either to *$C_3S$-type* (systems 1, 2, 3, 4) which produce few but large clusters of CH or to *PC-type* (systems 5, 6, 7) in which numerous smaller particles are identified. Mixes of $C_3S$ and gypsum (systems 2 and 4) show similar characteristics to pure $C_3S$: neither the number of CH clusters nor their morphological characteristics seem to be affected by the presence of gypsum. The situation is different in systems 5, 6 and 7 which all of which contain $C_3A$ and are very close to each other. Although system 5 (model mix of monophase $C_3S$ and $C_3A$) has an average particle size close to that of polyphase systems (model mix and PC), the mean number of CH particles is significantly lower (although still clearly different from the $C_3S$ type systems). This may be due to the fact that $C_3A$ is present as monophase grains and is thus more reactive (than when included in polyphase grains) or to the lower reactivity of gypsum due to its coarser size (compare to PC); either case may lead to a higher availability of aluminates in the system which may react with calcium ions and therefore inhibit or lower the nucleation of CH.

In $C_3S$ pastes the number of clusters slightly increases with time but remains very low compare to PC. Concerning the size of the clusters, the relative size increase for the PC system (7–19 µm) is comparatively much larger (25 times if one assumes a spherical shape) than for the C3S system (60–72 µm). As for the shape of particles, the form factor indicators show very little evolution for both systems.

The distributions of CH particle size (Fig. 6) also confirm the distinction between the two patterns of nucleation and growth. Systems containing $C_3A$ (5, 6 and 7) have similar characteristics with more than 75% of the particles being smaller than the

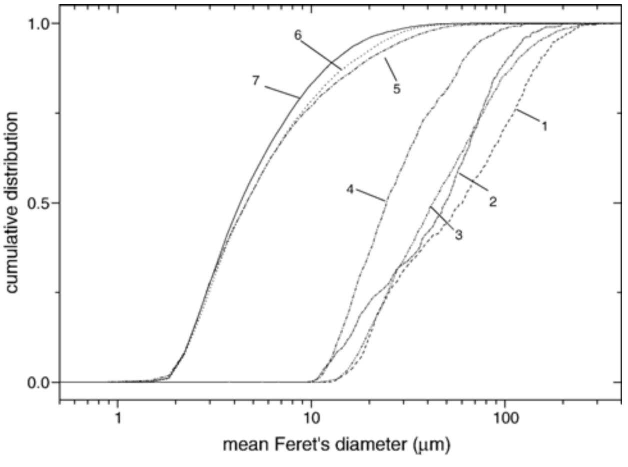

Fig. 6. CH particle size distribution (numbers correspond to systems in Table 1).

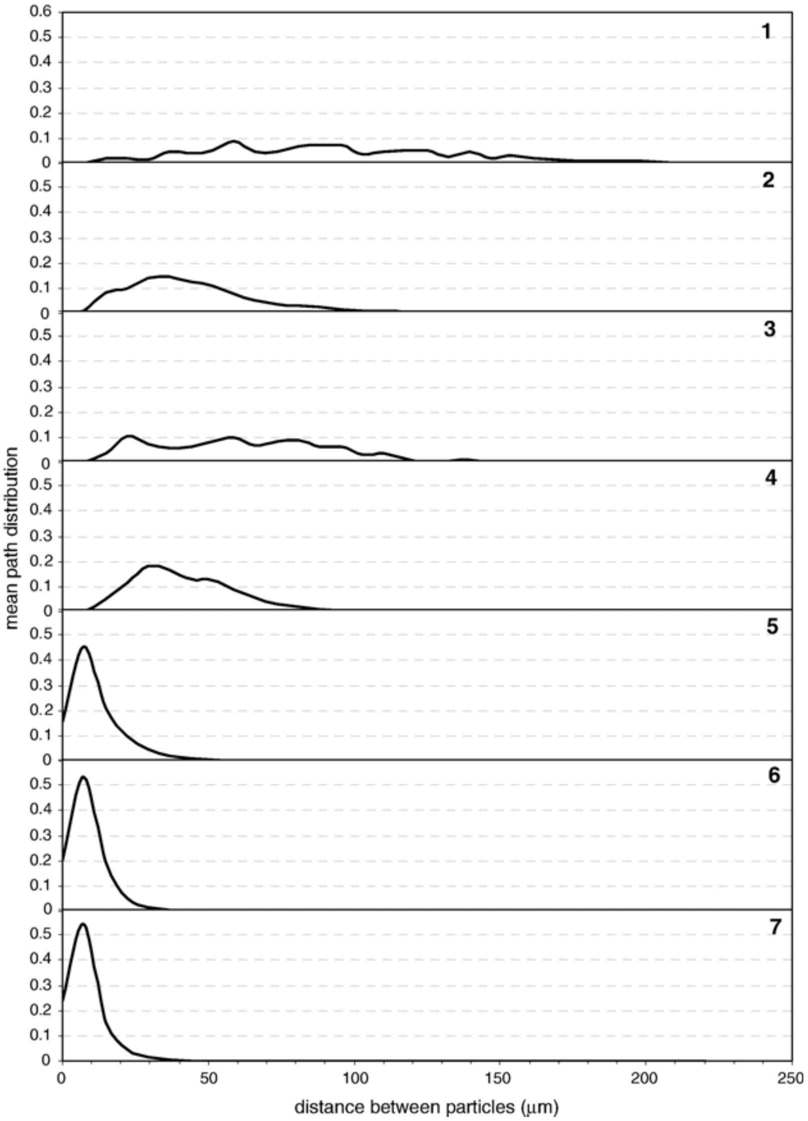

Fig. 7. Distribution of the mean free distance between the two closest CH particles.

smallest ones in the others 4 systems. $C_3S$ systems containing calcium sulfate (2 and 4) seem to have a slightly smaller minimum particle size compared to the $C_3S$ systems without sulfate (1 and 3).

The analysis of the mean distance between CH particles (Fig. 7) shows a narrower distribution for the PC system (CH particles are closely and evenly distributed in the matrix) and a large scattering of distances for the $C_3S$ system (random nucleation of clusters). The other mixes show one of these two characteristics according to the classification previously identified. The mean free distance of $C_3S$ systems containing gypsum (systems 2 and 4) show a slight influence of calcium sulfate which was not observed qualitatively: namely, that when gypsum is added to the mix, the distribution of distances is less scattered i.e. CH clusters are distributed more evenly in the matrix. This shows that even if the action of sulfates is not as important as in mixes containing aluminates as well, it nevertheless has a slight effect on the crystallisation of CH.

Concerning alkali ions, they have a very limited, although detectable, influence (Fig. 7) on the distribution of CH particles within the matrix, although given the scatter in the data, not hypothesis on the possible reasons for any difference is presented here. More interesting is the possible synergetic influence of sulphate and alkali (system 4): Table 3 and Figs. 6 and 7 show a significant difference in behaviour which has not been investigated here since the effect remains slight compared to the addition of aluminate ions.

### 3.3. Discussion

From the comparative study of pure $C_3S$ and PC hydration (Section 3.1), it was observed that CH clusters seem to have a preference to crystallise in the neighbourhood of calcium sulfate grains. It was even seen that CH sometimes seems to grow directly from the surface of gypsum (Fig. 3a) and this suggests that gypsum could act as CH nucleus. However, since the space group of CH (trigonal) is not compatible with any of those of calcium sulfates (gypsum-monoclinic, hemihydrate-orthorhombic, anhydrite-orthorhombic), the preferential nucleation next to gypsum crystals is unlikely to be epitaxial. Despite this apparent role of gypsum, overall the distinction between one pattern of nucleation and growth and another seems to be, by far the most, strongly related to the presence of the aluminate phase. It was not possible to study the hydration of systems containing calcium aluminate and no calcium sulfate due to the occurrence of flash set, when aluminate hydrates without gypsum.

Some studies [14] have shown that the aqueous phase of hydrating cement pastes is supersaturated with respect to CH and gypsum from the very first minutes of hydration. A saturation factor of 2–3 was measured for CH and remained constant for several hours whereas that of gypsum was 1.5 in the first minutes but then rapidly decreased to 1. No particular interaction between the saturation factors of gypsum and CH has been reported. Concerning the growth of CH crystals, Gartner [14] stated that the early supersaturation of a cement paste relative to CH ‘suggests that the crystallisation of portlandite is somewhat hindered at early ages’, and the author attributed this effect to surface poisoning of growing CH nuclei although he does not give any suggestion as to the origin of this poisoning.

In cement pastes with a low water to cement ratio, local concentration gradients may arise, but these are impossible to measure in real systems. Nevertheless, from this study it can be suggested that some feature of the local environment of gypsum crystals favours the precipitation of CH. This could be a higher concentration of calcium ions, due to the dissolving gypsum, or the absence of species which poison the growth in other regions. The two main candidates for poisoning CH nucleation are silicate or aluminate ions. Silicate ions are known to produce this effect [15] since they can absorb on the Ca-O sheets, as in C–S–H. It is known that the presence of alumina inhibits the reaction of calcium silicates [16] and probably suppresses the already low concentration of silicate ions in solution; but alumina itself may also poison CH nucleation. Thus, in a system with alumina and gypsum, there may be less silicate ions in general and very low concentrations of alumina around the gypsum grains, such that CH nucleation is favoured. Another possible explanation for the coupled effect of gypsum and alumina is that the consumption of some sulfate by reaction with alumina leads to more dissolution of gypsum, which increases slightly the supersaturation with respect to CH. However, at this stage these explanations are rather speculative.

## 4. Conclusion

Several model systems of hydrated cement phases have been studied by means of Scanning Electron Microscopy imaging and morphological image analysis in order to understand the occurrence and development of CH in cementitious systems. It has been shown that CH crystallises according to two main patterns:

- the first, *$C_3S$ type*, generates few, large, convoluted and randomly distributed clusters,
- the second, *PC type*, only observed in the presence of $C_3A$ and gypsum, produces numerous small particles, evenly and closely distributed in the matrix, and with two characteristics shapes: random clusters precipitating in empty constrained space and thin hexagonal platelets.

Study of the hydration of $C_3S$ and PC within the first 24 h indicates that locally gypsum seems to promote CH nucleation in the case of PC.

As a conclusion of this study, the growth of CH as in the PC type systems seems to be the result of a specific interaction between the availability of gypsum and alumina. Alkali ions by themselves seem to have a limited effect, but a synergetic influence may exist with sulfates.

## Acknowledgements

The authors thank Christian Vernet and Hélène Di Murro from Lafarge LCR for their helpful advice in synthesising the model phases.

## References

[1] J. Skalny, J. Gebauer, I. Odler (Eds.), Material Science of Concrete, Special Volume: Calcium Hydroxide in Concrete, The American Ceramic Society, Westerville, 2001.

[2] F.P. Glasser, The role of $Ca(OH)_2$ in Portland cement concretes, in: J. Skalny, J. Gebauer, I. Odler (Eds.), Material Science of Concrete, Special Volume: Calcium Hydroxide in Concrete, The American Ceramic Society, Westerville, 2001, pp. 11–35.

[3] S.Y. Hong, (2000), Calcium silicate hydrate: crystallisation and alkali sorption, PhD thesis, University of Aberdeen.

[4] M. Paul, F.P. Glasser, Impact of prolonged warm (85 °C) moist cure on Portland cement paste, Cement and Concrete Research 30 (12) (2000) 1869–1877.

[5] D.L. Kantro, S. Brunauer, C.H. Weise, Development of surface in the hydration of calcium silicates. II—Extension of investigations to earlier and later stages of hydration, Journal of Physical Chemistry 66 (1962) 1804–1809.

[6] H.G. Kurczyk, H.E. Schwiete, Concerning the hydration products of $C_3S$ and b-$C_2S$, Proc. 4th Int. Symp. Chem. Cem, p1.

[7] J.D. Birchall, N.L. Thomas, The mechanism of retardation of setting of OPC by sugars, Proceedings of the British Ceramic Society 35 (1984) 305–315.

[8] I.G. Richardson, Tobermorite/jennite- and tobermorite/calcium hydroxide-based models for the structure of C–S–H: applicability to hardened pastes of tricalcium silicate, β-dicalcium silicate, Portland cement, and blends of Portland cement with blast-furnace slag, metekaolin, or silica fume, Cement and Concrete Research 34 (2004) 1733–1777.

[9] J.J. Thomas, J.J. Chen, H.M. Jennings, D.A. Neumann, Ca–OH bonding in the C–S–H gel phase of tricalcium silicate and white Portland cement pastes measured by inelastic neutron scattering, Chemistry of Materials 15 (2003) 3813–3817.

[10] S. Diamond, Calcium hydroxide in cement paste and concrete-a microstructural appraisal, in: J. Skalny, J. Gebauer, I. Odler (Eds.), Material Science of Concrete, Special Volume: Calcium Hydroxide in Concrete, The American Ceramic Society, Westerville, 2001, pp. 37–58.

[11] K.O. Kjellsen, H. Justes, Revisiting the microstructure of hydrated tricalcium silicate—a comparison with Portland cement, Cement and Concrete Composites 26 (2004) 947–956.

[12] J.C. Russ, Practical Stereology, 2nd edition, Plenum press, New-York, 1991.

[13] P.E. Stutzman, Scanning Electron Microscopy in concrete petrography, in: J. Skalny, J. Gebauer, I. Odler (Eds.), Material Science of Concrete, Special

Volume: Calcium Hydroxide in Concrete, The American Ceramic Society, Westerville, 2001, pp. 59–72.

[14] E.M. Gartner, F.J. Tang, S.J. Weiss, Saturation factors for calcium hydroxide and calcium sulfates in fresh Portland cement pastes, Journal of the American Ceramic Society 68 (1985) 667–673.

[15] Z.-Q. Wu, J.F. Young, Formation of calcium hydroxide from aqueous suspensions of tricalcium silicate, Journal of the American Ceramic Society 67 (1984) 48–51.

[16] P. Gu, J.J. Beaudoin, E.G. Quinn, R.E. Myers, Early strength development and hydration of ordinary Portland cement/calcium aluminate cement pastes, Advanced Cement Based Materials 6 (2) (1997) 53–58.